QUANTIFYING VARIABILITY OF RECYCLED FIBRES IN COMPOSITES USING MULTILEVEL MONTE CARLO

T. J. Dodwell[1], K. E. Evans[1], O. Ghita[1], A. S. Sandhu[1], L. Savage[1]

[1]College of Engineering, Mathematics and Physical Sciences, University of Exeter, Exeter, EX4 4PY
Emails: t.dodwell@exeter.ac.uk, o.ghita@exeter.ac.uk, as909@exeter.ac.uk, l.savage@exeter.ac.uk

Keywords: Recycled Fibres, SMC, Multilevel Monte Carlos, Random Fibre Architectures, Finite Elements.

Abstract
This paper presents a novel sequence of computational methodologies to efficiently quantify the variability in mechanical properties of composites remanufactured from recycled/recovered fibres. This model is broken up into three steps. Firstly, we describe a method for generating realistic random fibre architectures using random walks. This stochastic model is parameterised by distributions for fibre length, fibre radius and stiffness; whilst the random fibre paths are driven by a multivariate von Mises-Fisher distribution, which controls anisotropy and local fibre bending. Secondly, we describe a 3D rebar finite element for random fibres along with the homogenisation procedures required to compute macroscale stiffness properties for a given random fibre realisation. The third and final step details a novel multilevel Monte Carlo (MLMC) methodology, a way of combining a hierarchy of model resolutions, to efficiently calculate the distribution of the macro properties desired. Numerical experiments, parameterised by real data from a fibre recover processes (Mechanical Grinding) demonstrate the potential of the methods described. In particular MLMC demonstrates gains of as much as 15-fold computational speed-up over standard Monte Carlos methods. Importantly such efficient methods allow better prediction of performance and encourage the use of recycled fibres back into new composites.

1. Introduction

Thermoset composites of polyester resin combined with short, randomly orientated fibres are extensively used for high volume, lower cost applications such as sheet moulding compounds (SMC). The increasing cost of landfill and environmental impact means there is an ever increasing pressure to recycle composites [1,2].Several technologies (e.g. Mechanical Grinding [3], High Voltage Fragmentation [3], solvolysis[4]) have been developed for recovery of fibre fractions yet low material quality [3] and prohibitively large recovery costs remain obstacles for significant commercial uptake [1,2]. If such materials are to be reused in advanced applications, an important step is to understand and control variability in their mechanical properties.

The variability in performance of recycled fibres has largely been characterized experimentally in terms of macro stiffness and strength, reinforcement architecture , local fibre and interfacial properties[1]. However, there is little modelling which focuses on the stochastic nature of the recycled short, discontinuous, fibre architectures, their remanufacturing as a SMC and the relation to macroscale properties. A recent set of experimental study which compared mechanical properties of SMCs made with recovered glass fibres from two different recycling processes (Mechanical Grinding and HV Fragmentation). The results shows that the recovered fibre length distribution (Fig.1 (left)) had a non-trivial link to flexural stiffness Fig. 1 (right). This is particularly highlighted when the flexural stiffness was estimated for

Excerpt from ISBN 978-3-00-053387-7

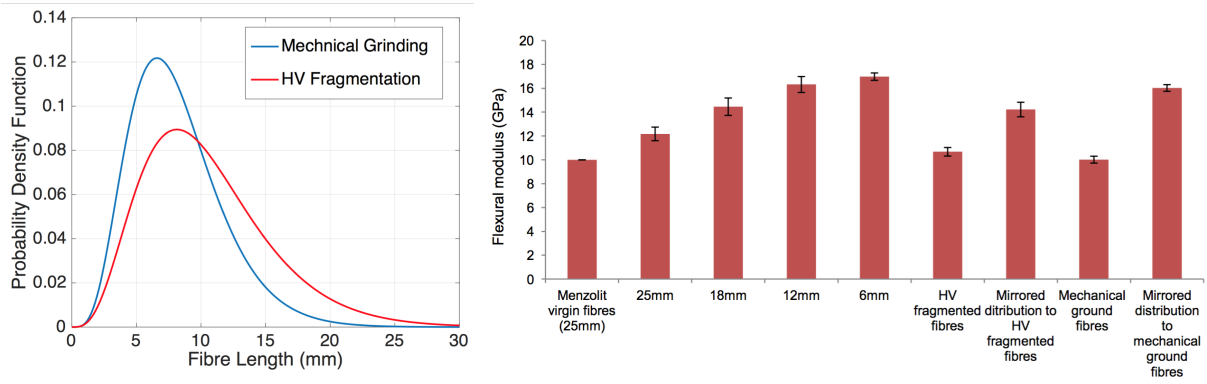

Figure 1. (Left) Fibre length distribution from two fibre recovery processes. (Right) Flexural stiffness of SMC with different length fibres / fibre distributions.

SMCs made from virgin fibres with artificially generate length distributions, as shown in Fig. 1 (right). In particularly we note that even though the fibre volume fraction for each composite is the same, SMC with 6*mm* fibres demonstrate a statistically significant higher stiffness than SMCs made with longer fibres (e.g. 25mm). This demonstrates that estimating the macroscale properties is more complex than a simply rule of mixtures. This experimental work has motivated the modelling question 'What steps are required to model recycled composites to access the functional relationship between the stochastic distribution of random inputs of the recovered fibres (such as fibre length, stiffness and an isotropy) and the SMC resin with the their macroscale properties?' In this paper we make the initial modelling steps to answer this question.

Classical methods for investigating uncertainty consider how variability in inputs propagate through a model by simply averaging the output of many independent samples (Monte Carlo). For many applications a single realisation is expensive, yet many samples are required due to possible number of fibre configurations; making standard algorithms computationally expensive. Here we implement a Multilevel Monte Carlo (MLMC) method to achieve efficient estimation of macro properties of recycled composites. The MLMC method was first suggested in the context of option pricing in financial mathematics [6]. MLMC's huge potential in uncertainty quantification for engineering applications was identified by Cliffe et al.[5] in particular for subsurface hydrology applications. Since then, it has been applied to other applications, including random defects in aerospace composites [7], and has also been extended to account for experimental data within a Bayesian setting [8]. The method achieves large speed-ups by combining a hierarchy of model fidelities, so that only a few costly fine scale computations are needed to accurately estimate the distribution of macro-scale properties.

The model in this paper requires three steps. Firstly, we need to develop a method to generate realistic representative volume elements (RVE) of the random fibre architecture from experimental data on fibre length distribution, orientation and fibre quality. For each realisation, the centre-line of cylindrical fibres are described by Markov processes driven by a von Mises-Fisher (vMF) distribution with parameters that control the average fibre direction and fibre bending stiffness. Variability in the SMC resin/paste arising through porosity defects are introduced to the model using correlated random fields. Secondly, a hierarchy of finite element modes of the RVE are constructed, for which the random fibres are models are stiff rebar inclusions. For each realisation, on any grid resolution, computational homogenization is applied to compute effective macro properties for each sample. Finally the MLMC algorithm combines many coarse solutions with fewer detailed, in an optimal ratio, to obtain robust estimates and bounds for the mechanical properties. After detailing the methods, and giving a general introduction to the

Excerpt from ISBN 978-3-00-053387-7

stochastic methods (in particular MLMC), the paper concludes with a number of numerical experiments, which we demonstrates the methodology with random inputs parameterised from measured data from two recycling processes (Mechanical Grinding and HV Fragmentation). Finally we point to future steps to validate the methodologies for practical (structural) applications for recycled composites.

2. Modelling Recycling Composites

In this section we first describe how we generate random fibre architectures on a periodic cube $\Omega := [0, L]^3$, followed by a brief description of the finite element procedure used to model the random fibre composite.

2.1. Generating random fibre architectures and porosity defects

The aim is to generate realistic random fibre architectures on a periodic cube $\Omega := [0, L]^3$ made up of fibres with a length distribution of those measured from the recycling processes Fig. 1. This paper parameterises random fibre lengths by a Gamma distribution, $\ell \sim \Gamma(k, \theta)$ with mean $\mathbb{E}[\ell] = k\theta$ and variance $\mathbb{V}[\ell] = k\theta^2$. However in general any distribution could be used. Assuming each fibre has a radius r_f and therefore an average volume $\frac{1}{2}\pi r_f^2 \mathbb{E}[\ell]$, to achieve a target fibre volume fraction of V_f we generate $N = 2L^3 V_f / \pi r_f \mathbb{E}[\ell]$.

To generate the j^{th} fibre, we firstly sample a random length ℓ_j from $\Gamma(k, \theta)$. The position of the fibre is then described by a set of $M_j = \lceil \ell_j / \Delta\ell \rceil$ discrete points in $\mathbb{R}^3$, $X^{(j)} = \{\underline{x}_0^{(j)}, \underline{x}_1^{(j)}, \ldots, \underline{x}_{M_j}^{(j)}\}$, where $\Delta\ell$ is the distance (in $\mathbb{R}^3$) between consecutive points. Randomly positioning the first point $\underline{x}_0^{(j)}$ in Ω using a uniform distribution for each component on $[0, L]$, subsequent points in the fibre are generated by the Markov process, $\underline{x}_{i+1}^{(j)} = \underline{x}_i^{(j)} + \Delta\ell \ \underline{\mu}_i^{(j)}$. Here the random directional vector $\underline{\mu}_i^{(j)}$ is generated from a multi-variant von-Mises Fisher (VMF) distribution with a probability density function

$$f_p(\underline{\mu}; \kappa, \underline{\mu}^*) = \frac{\kappa}{4\pi \sinh \kappa} \exp(\kappa \underline{\mu}^{*T} \underline{\mu}), \quad \text{where } \kappa = |\kappa_1 \mu_1 + \kappa_2 \mu_2| \quad \text{and} \quad \underline{\mu}^* = \frac{\kappa_1 \mu_1 + \kappa_2 \mu_2}{\kappa}. \tag{1}$$

The parameters $\underline{\mu}^* \in \mathbb{R}^3$ and $\kappa \in \mathbb{R}^+ \backslash \{0\}$ define the *mean direction* and *concentration factor* respectively, so that the greater the value of κ the more concentrated the samples are on the mean direction $\underline{\mu}^*$, as demonstrated in Fig 2 . In this paper $\underline{\mu}^*$ and κ are the weighted average of two 'mean' directions ($\underline{\mu}_1$ and $\underline{\mu}_2$) and associated concentrations factors κ_1 and κ_2. For generating the random fibre we set $\underline{\mu}_1$ to be the expected direction of the overall laminate (e.g. for uni-directional laminates $\mu_1 = [1, 0, 0]^T$) whilst $\underline{\mu}_2$ is set equal to the direction at the previous point i.e. $\underline{\mu}_{i-1}^{(j)}$. Therefore the concentration factor κ_1 controls how well aligned the fibres are with a prescribed direction, whilst κ_2 controls the level of fibre deviation (or bending). Figure 2 (left) shows random fibre architectures with different a concentration factors and $\underline{\mu}_1 = [1, 0, 0]^T$.

Spatial variability random porosity are introduce into the SMC resin using a truncated Karhunen-Loeve (K-L) expansion to define the function $\iota(\underline{x}) = \sum_{i=1}^{\infty} \sqrt{\lambda_i} \xi_i^{(k)} f_i(\underline{x})$. Here $\{\xi_i\}$ is a set of Gaussian random variables such that $\xi_i \sim N(0, \sigma_{kl})$; and $\{(\lambda_i, f_i)\}$ is the set of eigenvalue/function pairs of the exponential covariance function $C(x, y) = \exp(|\underline{x} - \underline{y}| / \ell_{kl})$ where $\ell_{kl} \in \mathbb{R}^+$ defines the *correlation length* of the porosity defects. The Young's modulus of the resin is set so that

$$E_r(\underline{x}) = 0 \quad \text{if} \quad \iota(\underline{x}) < -\beta\sigma_{kl} \quad \text{else} \quad E_r(\underline{x}) = \mathbb{E}[E_r] + \frac{\sigma_r}{\sigma_{kl}} \iota(\underline{x}), \tag{2}$$

where $\sigma_{kl} = \sqrt{\sum_{i=1}^{N} \lambda_i}$. To achieve on average 1% porosity defects we set $\beta = 1.96$ (one-sided confidence interval). Figure 2 (right) shows typical porosity defect (with a higher % than normal) generated by the K-L modes.

Excerpt from ISBN 978-3-00-053387-7

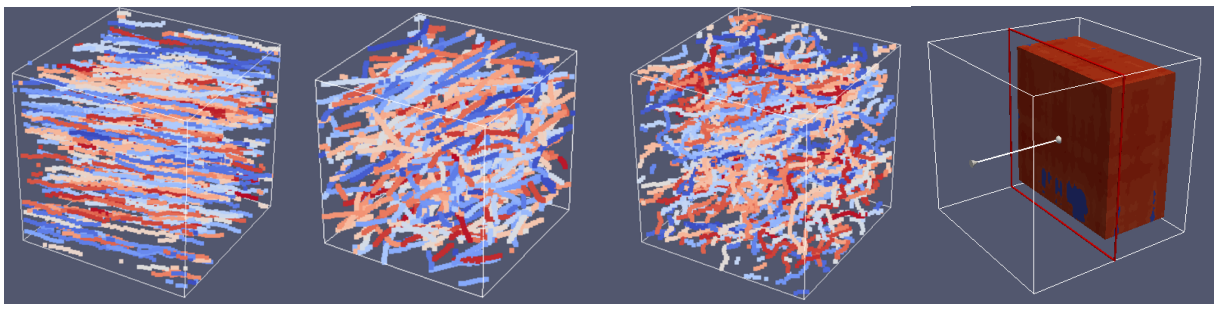

Figure 2. (Left) Three random realisation of fibre architectures with different vMF parameters, with decreasing anisotropy and average fibre length from left to right.(Right) Slice through resin, blue shows porosity defect. Example has higher porosity for demonstration (12%) and $\ell_{kl} = 0.1$mm.

2.2. Finite element Formulation

Modelling a network of stiff fibre inclusions is challenging for two principle reasons. Firstly the aspect ratio of the fibre is approximately 1 : 1000 (diameter to length), therefore a finite element representation of a single fibre would require a prohibitively large number of elements. Secondly, the material contrast between the fibre and resin is large (∼ a factor of 10), leading to complex local stress distributions / gradients. In this paper we address the first challenge by modelling fibres as stiff 1D dimensional inclusions, as is often done for modelling steel reinforcements in concrete (e.g. rebar elements). As for the second challenge, for now we assume that the resin and fibre are perfectly bonded and strain together.

The deformation of our recycled composite is defined by the vector displacement field $\underline{u}(\underline{x}) = [u, v, w]^T$ on Ω, with corresponding small strain measure / tensor $\varepsilon(\underline{u}) = \frac{1}{2}\left(\nabla\underline{u} + \nabla\underline{u}^T\right)$. Material strains are connected to stresses in the resin via an isotropic elastic tensor such that $\sigma_r = \mathbf{D}_r(\underline{x})\varepsilon$, which depends on $E_r(\underline{x})$ and ν_r the (locally varying) Young's Modulus and poisson ratio of the resin respectively. For the fibre reinforcement, we assume it is in a purely axially stressed state and there exists perfect bonding between the fibre and the resin. Thus the local axial strain field ε'_{xx} can be determined directly from the macro scale strain ε such that

$$\varepsilon'_{xx} = \mu_1^2\varepsilon_{xx} + \mu_2^2\varepsilon_{yy} + \mu_3^2\varepsilon_{zz} + \mu_1\mu_3\varepsilon_{zx} + \mu_2\mu_3\varepsilon_{yz} + \mu_1\mu_2\varepsilon_{xy}, \tag{3}$$

where $\underline{\mu} = [\mu_1, \mu_2, \mu_3]^T$ are the local direction cosines of the fibre (as define in the previous section). Of all the six stress components in the fibre only the σ'_{xx} is not zero, so that $\sigma'_{xx} = E_f\varepsilon'_{xx}$, where E_f is the Young's Modulus of the fibre.

Subjected to a mixture of displacement (Dirichlet) and stress (Neumann) boundary conditions, stress equilibrium (in the absence of body forces) is given by the system of equations

$$\nabla\cdot\sigma = \underline{0} \quad \text{with} \quad \underline{u}(\underline{x}) = \underline{h} \quad \text{for} \quad \underline{x} \in \partial\Omega_{\text{Dir.}} \quad \underline{\sigma}\cdot\underline{n} = \underline{g}(\underline{x}) \quad \text{for} \quad \underline{x} \in \partial\Omega. \tag{4}$$

where $\underline{n}$ denotes the normal to the boundary of Ω denoted $\partial\Omega$, and $\nabla\cdot$ the divergence operator. To solve (3) with the finite element method (FEM) the system of differential equations (3) is recast in variational (or weak) form, so that

$$a(\underline{u}, \underline{v}) + \mathcal{L}(\underline{v}) = \int_\Omega \mathbf{D}\ \varepsilon(\underline{u}) : \varepsilon(\underline{v})\ dV + \int_{\partial\Omega} \sigma\cdot\underline{n}\ d\underline{x} = 0. \tag{5}$$

This equation holds for any variation $\underline{\hat{u}}$ in a suitable function space V. The solution $\underline{u}$ is also sought in V - here the Sobolev space H^1, the set of all square integrable functions, with square integral first derivatives,

Excerpt from ISBN 978-3-00-053387-7

satisfying the displacement boundary conditions. To approximate the $\underline{u}$ the domain is discretised into a structured (hexahedron) grid $\mathcal{Q}_h = \{\Omega_e^{(i)}\}_{i=1}^{\text{nel}}$, where nel is the number of elements, nvert the number of vertices and h the largest dimension of the elements. The solution to (4) is approximated by restricting displacements to the finite dimensional (vector) subspace $V_h \subset V$ of continuous piecewise linear vector functions in $\mathbb{R}^3$. For which each component of the displacement at the vertices is interpolated across the domain with a set of piecewise linear shape functions $\{\phi_i(\underline{x})\}_{i=1}^{\text{nvert}}$.

For a given random sample, a preprocessing steps first assign fibres (or part of fibres) to each finite element and compute the local fibre volume fraction within each element V_f. The integration of the element stiffness matrix is then split between the resin and fibre reinforcements, so that for a given element and in matrix form the first term of (4) becomes

$$\mathbf{K}_e = \int_{\Omega_e^{\text{resin}}} \mathbf{B}_e^T \mathbf{D}_r \mathbf{B}_e \, dV_{\text{resin}} + \sum_{i=1}^{\#\text{fibres}} \frac{1}{2}\pi r_f^2 \int_{\ell_i} \mathbf{B}_e^T \left[\mathbf{T}^T \mathbf{D}_f \mathbf{T}\right] \mathbf{B}_e d\ell_i. \tag{6}$$

Here $\mathbf{B}_e$ is the strain-displacement matrix which maps vertex displacements to strains with in an element, $\mathbf{D}_r$ and $\mathbf{D}_f$ are the elasticity matrices for the resin and fibre respectively, and $\mathbf{T}$ is the transformation matrix of the strains from local to global coordinates (i.e. (2) rewritten in matrix form). In practice the integral in both terms of (5) are computed using quadrature. Since (3) is a 3D vector equation, the total global degrees of freedom are $M = 3\text{nvert}$. Therefore for any standard finite element calculation, element stiffness matrices (5) can be combined into a single global stiffness matrix of the form $\mathbf{K}\underline{d} = \underline{f}$ where $\mathbf{K} \in \mathbb{R}^{M\times M}$ is the (sparse) global stiffness matrix and $\underline{f} \in \mathbb{R}^M$ is the load vector due to the prescribed boundary conditions, and the solution vector $\underline{d} \in \mathbb{R}^M$ contains the displacements at each vertex. All calculations, including the preprocessing steps for generating the fibres and the monte carlo algorithm described in the section which follows, have been written in a bespoke code in `c++`. In particular for the finite element calculation, the code utilises the high performance finite element library DUNE [9]. A general framework which provides easy access to state of numerical solvers.

In this paper we are interested in computing the *effective* macroscale properties of the recycled composites. That is if Σ_{ij} and E_{ij} denote the (symmetric) macroscale stress and strain tensors, we wish to calculate elements of the *effective* macroscale elastic tensor C_{ijkl} such that $\Sigma_{ij} = C_{ijkl}E_{kl}$. To do this we seek solutions of the form $\underline{u}(x) = \mathbf{E}\underline{x} + \underline{u}^{\text{per.}}(\underline{x})$,where the symmetric matrix $\mathbf{E}$ containing macroscale strain values, and $\underline{u}^{\text{per.}}$ is a displacement field which is periodic on the boundary of Ω such that $\underline{u}^{\text{per.}}(\underline{0}) = \underline{0}$ (to prevent rigid body modes). To calculate values C_{ijkl}, we set $E_{kl} = E_{kl} = 1$ and all other values to zero. Using finite elements we then calculate the corresponding force, $a(\underline{u}^*, v)$, to achieve the displacement $\underline{u}^*$ on each vertex. This force then is the load vector $\mathcal{L}(v)$ in (4), and we solve for the periodic perturbation $\underline{u}^{\text{per.}}$. Written mathematically this is, find $\underline{u}^{\text{per.}}$ such that $a(\underline{u}^{\text{per.}}, v) + a(\underline{u}^*, v) = 0$. Noting that $\Sigma_{ij} = |\Omega|^{-1}\int_\Omega \sigma_{ij}(\underline{u})\, d\Omega$, the effective macroscale stiffness is given by $C_{ijkl} = \Sigma_{ij}/E_{kl}$.

3. Multilevel Monte Carlos Methodology and Implementation

The aim is to quantify the distribution of a particular macro-scale property (e.g. C_{ijkl}). From the model formulation presented the simplest way to do this is Monte Carlos, in which we calculate the quantity of interest $Q = C_{ijkl}$ for N independent samples on a FEM grid with M degrees of freedom, and estimate the expected value $\mathbb{E}[Q]$ and variance $\mathbb{V}[Q]$ of Q via

$$\mathbb{E}[Q] \approx \hat{Q}_{M,N}^{MC} = \frac{1}{N}\sum_{i=1}^{N} Q_M^{(i)} \quad \text{and} \quad \mathbb{V}[Q] \approx s^2 = \frac{1}{N}\sum_{i=1}^{N}\left(Q_M^{(i)} - \widehat{Q}_{M,N}^{\text{MC}}\right)^2. \tag{7}$$

Excerpt from ISBN 978-3-00-053387-7

For this estimate we quantity the its error, defined by the root mean square error (RSME) $e(\hat{Q})$, given by

$$e(\hat{Q}_{M,N})^2 = \frac{\mathbb{V}[Q_M]}{N} + \mathbb{E}[Q_M - Q]^2 \tag{8}$$

We see the RSME is made up of two terms. The first quantifies the sampling error, which arises from approximating $\mathbb{E}[Q]$ with only a finite number of samples. The second term represents the FEM error arising from approximating Q by Q_M, the solution of (4) on a finite dimensional grid. To produce sufficiently small errors in our approximation of $\mathbb{E}[Q]$ we need a large number of samples N each computed on a sufficiently fine (and costly to solve) finite element grid. For this application, we will see that standard Monte Carlo methods quickly become computationally unfeasible. To overcome we introduce a hierarchy of computational grids, coarse cheaper, less accurate grids to fine, expensive, accurate ones, Fig. 3 . We let L denote the maximum level, and grid levels $\ell = 0 \dots L$ have M_ℓ degrees of freedom. The aim is to combine simulations across all grids, so that most the computations are done on the cheaper, coarser levels; whilst we still obtain the accuracy of the predictions on the finer grids.

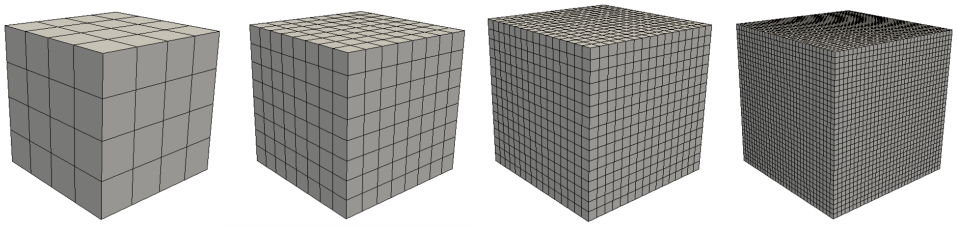

Figure 3. A typical hierarchy of computational grids used for MLMC. Here the coarsest grid $\ell = 0$ has $M_0 = 192$ degrees of freedom, the finest $\ell = L = 3$ has $M_3 = 107,188$.

Here we use the Multilevel Monte Carlo Method (MLCMC). The mathematical trick in this methods is to exploit the linearity of a expectation operator i.e. $\mathbb{E}[A + B] = \mathbb{E}[A] + \mathbb{E}[B]$. Therefore the expected value on a fine grid can be rewritten as follows

$$\mathbb{E}[Q_{M_l}] = \mathbb{E}[Q_{M_l} - Q_{M_{\ell-1}} + Q_{M_{\ell-1}}] = \mathbb{E}[Q_{M_{\ell-1}}] + \mathbb{E}[Q_{M_l} - Q_{M_{\ell-1}}], \tag{9}$$

i.e. the expected value on a coarser grid, plus the expected value of the difference between the coarse and fine grid. If we denote the random variable $Y_\ell = Q_{M_l} - Q_{M_{\ell-1}}$ such that $Y_0 = Q_{M_0}$, we can repeat this process of all L levels so that $\mathbb{E}[Q_M] = \sum_{\ell=0}^{L} \mathbb{E}[Y_\ell]$. As for standard monte carlos, expected values on each level $\mathbb{E}[Y_\ell]$ can be approximated by $\hat{Y}_\ell^{MC}$ as define by (7). The multilevel approximation has RSME error $\sum_{\ell=0}^{L} \mathbb{V}[Q_\ell]/N_\ell + \mathbb{E}[Q_{M_L} - Q]^2$. Importantly we note that the variances of differences (i.e. $V_\ell = \mathbb{V}[Y_\ell]$ for $\ell > 0$) are much smaller than variances of the quantities themselves $\mathbb{V}[Q_\ell]$; therefore on the higher (or finer grid) levels we need many fewer samples to achieve a given sampling error. If C_ℓ denote the computational cost (in secs) on a single sample on level ℓ, then if N_ℓ samples are done on level ℓ, the total computational of the algorithm is $\sum_{\ell=0}^{L} N_\ell C_\ell$. If we minimise this total cost subject to the constraint that the total RSME is ϵ, the optimal samples on each level are

$$N_\ell = \frac{2}{\epsilon^2} \left(\sum_{i=0}^{L} \sqrt{V_i C_i} \right) \sqrt{\frac{V_\ell}{C_\ell}}. \tag{10}$$

In practice, to achieve a given RSME for our estimate, we can be computed N_ℓ and L "on the fly" from the sample averages and the sample variances of Y_ℓ. For details of how the MLMC algorithm can be implemented see [7]. We do note that since each sample is independent the process is readily parallelized by (equally) distributing samples across each available processor.

Excerpt from ISBN 978-3-00-053387-7

4. Results - Demonstration of Methodology

In this section we briefly demonstrate the methodology proposed for a simple example for which we compute the effective macroscale stiffness C_{1111} for a SMC made with recovered fibres from the mechanical grinding process, as described in [3]. Calculations are on a periodic domain $\Omega = [0, 1\text{mm}]^3$, with a target fibre volume fraction $V_f = 25\%$. From experimental measurements of recovered fibres for the mechanical grinding process [3] we take the following distributions for material properties

$$\ell \sim \Gamma(4.48, 1.82\text{mm}), \quad E_f \sim N(55.91\ \text{GPa}, 16.90\ \text{GPa}) \quad \text{and} \quad r_f \sim N(7.75\mu m, 0.84\mu m) \tag{11}$$

Local variability in resin properties across these samples are captured with 1000 KL modes (10 in each dimension) with a correlation length 1mm, for which the Young's Modulus of the resin $E_r = 4.0$GPa, $\sigma_r =$ and the cut-off parameter for a porosity defect $\beta = -1.96$, which corresponds to on average a 1% porosity in samples typical for SMC composite. For these numerical test the ν_r is taken as the fixed value 0.25. Finally the VMF fisher distribution parameters are fixed at $k_1 = 5$ and $k_2 = 20$. For all calculations computation level 0 has 4 elements in each direction (64 in total) subsequent level as achieved by uniform refinement (Fig. 3). All results presented are computed to a RSME of 0.5%.

Figure 4 (left) shows the average computational cost, for a single solve against degrees of freedom. For this numerical experiment we estimate an average macro $C_{1111} = 11.27$GPa, to do this we calculate 503 on the coarsest grid and only 6 samples on the most expensive grid (Fig. 4 (middle)). From this we can estimate the computational gain over using a standard Monte Carlos method of approximately 15 fold. We note that for even smaller RSME this factor grows. As noted in section 3 this gain comes from the variance reduction over the levels (Fig. 4 (right)), therefore many fewer samples are required on the expensive levels for a fixed sampling error.

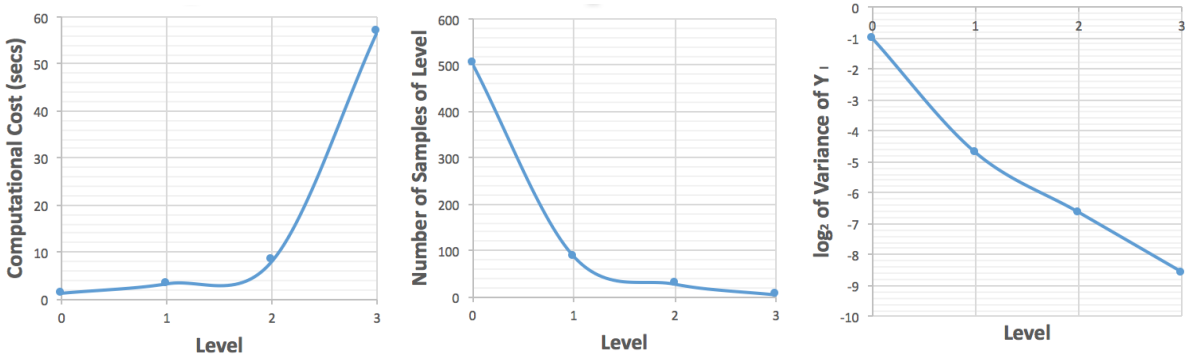

Figure 4. (Left) Degrees of freedom vs. Computational Cost. (Middle) MLMC samples per level. (Right) Demonstration of variance reduction across the levels.

5. Concluding Remarks & Future Work

This paper details a novel sequence of modelling steps, to quantify the variability in composite materials made from recovered fibres. Numerical experiments, parameterised by real data from a fibre recover processes (Mechanical Grinding) demonstrate the potential of the methods described. In particular MLMC demonstrates gains of as much as 15-fold computational speed-up over standard Monte Carlos methods. Importantly such efficient methods allow better prediction of performance and encourage the use of recycled fibres back into new composites. A clear route to increasing the business for recycling composites. For the values we have not computed flexural stiffness directly, however from data values of SMC tensile stiffness, the predicted values are within the typical range. Further work will (1) use the model access

Excerpt from ISBN 978-3-00-053387-7

the functional relationship between the stochastic distribution of random inputs of the recovered fibres and the SMC resin with the their macroscale properties. In particular unpick the non-trivial relationship between fibre length and stiffness as reported in the experiments. (2) Improve the multiscale models for failure of recycled composites rather than only stiffness. (3) Determine the VMF parameters (κ_1 and κ_2) from experimental data. (4) Estimation the complete random tensor, this is however more complex since the stiffness values are dependent, and the tensor itself must remain symmetric positive definite.

Acknowledgments

Work presented in this paper was supported by EPSRC grant EXHUME - Efficient X-sector use of HeterogeneoUs MatErials in Manufacturing (EP/K026348/1).

References

[1] S. Pimenta and S. T. Pinho, *Recycling carbon fibre reinforced polymers for structural applications: Technology review and market outlook* Waste Management, 31(2)378392, 2011.

[2] S. J. Pickering, *Recycling technologies for thermoset composite materials current status*, Composites Part A, 37(8)12061215, 2006.

[3] D. Rouholamin, Y.T. Shyng, L. Savage and O. Ghita. *A comparative study into mechanical performance of glass fibres recovered through mechanical grinding and high voltage pulse power fragmentation.* In: 16th European conference on composite materials, Seville, Spain, June, 2014.

[4] G. Oliveux, L. O. Dandy and G. A. Leeke, *Degradation of a Model Epoxy Resin by Solvolysis* Routes, Polymer Degradation and Stability, Polymer Degradation and Stability 118:96-103, 2015.

[5] K.A. Cliffe, M.B. Giles, R. Scheichl, and A.L. Teckentrup. *Multilevel Monte Carlo methods and applications to elliptic PDEs with random coefficients.* Computing and Visualization in Science, 14(1):3-15, 2011.

[6] M.B. Giles. *Multilevel Monte Carlo path simulation* .Operations Research, 56(3):981-986, 2008.

[7] R. Butler, T.J. Dodwell, T. Kim, S. Kynaston, R. Scheichl, R.T. Haftka, N.H. Kim. *'Uncertainty quantification of composite structures with defects using multilevel Monte Carlo simulations'.* Proceedings of the 17th AIAA Non-Deterministic Approaches Conference, 2014

[8] T. J. Dodwell, C. Ketelsen, R. Scheichl, and A. L. Teckentrup. *A hierarchical multilevel Markov chain Monte Carlo algorithm with applications to uncertainty quantification in subsurface flow.* SIAM/ASA J. Uncertain. Quantif., 3(1):10751108, 2015.

[9] P. Bastian, F. Heimann, S. Marnach Generic implementation of finite element methods in the distributed and unified numerics environment (DUNE) Kybernetika, 46(2), pp.294-315, 2010

Excerpt from ISBN 978-3-00-053387-7